

Batrachotoxin-modified Sodium Channels from Squid Optic Nerve in Planar Bilayers

Ion Conduction and Gating Properties

MARIA I. BEHRENS, ANDRES OBERHAUSER, FRANCISCO BEZANILLA, and
RAMON LATORRE

From the Centro de Estudios Científicos de Santiago, Casilla 16443 Santiago 9 Chile, Departamento de Biología, Facultad de Ciencias Universidad de Chile Santiago, Chile; and the Department of Physiology, Jerry Lewis Neuromuscular Research Center, Ahmanson Laboratory of Neurobiology, University of California, Los Angeles, California 90024

ABSTRACT Squid optic nerve sodium channels were characterized in planar bilayers in the presence of batrachotoxin (BTX). The channel exhibits a conductance of 20 pS in symmetrical 200 mM NaCl and behaves as a sodium electrode. The single-channel conductance saturates with increasing the concentration of sodium and the channel conductance vs. sodium concentration relation is well described by a simple rectangular hyperbola. The apparent dissociation constant of the channel for sodium is 11 mM and the maximal conductance is 23 pS. The selectivity determined from reversal potentials obtained in mixed ionic conditions is $\text{Na}^+ \sim \text{Li}^+ > \text{K}^+ > \text{Rb}^+ > \text{Cs}^+$. Calcium blocks the channel in a voltage-dependent manner. Analysis of single-channel membranes showed that the probability of being open (P_o) vs. voltage relation is sigmoidal with a value of 0.5 between -90 and -100 mV. The fitting of P_o requires at least two closed and one open state. The apparent gating charge required to move through the whole transmembrane voltage during the closed-open transition is four to five electronic charges per channel. Distribution of open and closed times are well described by single exponentials in most of the voltage range tested and mean open and mean closed times are voltage dependent. The number of charges associated with channel closing is 1.6 electronic charges per channel. Tetrodotoxin blocked the BTX-modified channel being the blockade favored by negative voltages. The apparent dissociation constant at zero potential is 16 nM. We concluded that sodium channels from the squid optic nerve are similar to other BTX-modified channels reconstituted in bilayers and to the BTX-modified sodium channel detected in the squid giant axon.

INTRODUCTION

A vast amount of information about sodium channels in the squid giant axon has been gathered since Hodgkin and Huxley (1952) gave the first quantitative de-

Address reprint requests to Dr. F. Bezanilla, Department of Physiology, University of California, Los Angeles, Los Angeles, CA 90024.

scription of the ionic currents mediated by these channels. In this preparation it is possible at present to study macroscopic, gating, and single-channel currents (Armstrong, 1981; Bezanilla, 1985*a*; Llano and Bezanilla, 1986; Bezanilla, 1987). Furthermore, the possibility of measuring gating currents together with measurements of macroscopic and single-channel currents make it possible to arrive at plausible models of the opening and closing of sodium channels. In this regard the squid axon preparation is quite unique, because measurements of gating currents in other preparations that allow single-channel recording is less likely to be successful due to their low channel density.

The techniques that allow the study of sodium channels in the isolated squid giant axon can be complemented with the information obtained by incorporation of sodium channels into planar lipid bilayers. This procedure allows the analysis of individual sodium channels under conditions in which it is possible to control the aqueous and lipid environment of the channel. Detection of sodium channels in planar bilayers is also the first step towards a purification and reconstitution of the functional pore-forming protein.

Using batrachotoxin (BTX), a steroidal alkaloid known to remove the inactivation process (for review, see Khodorov, 1985), sodium channels from rat and dog brain, and skeletal muscle membranes have been characterized by incorporation into planar bilayers (Krueger et al., 1983; Moczydlowski et al., 1984*a, b*; Green et al., 1984, 1987*a, b*). Furthermore, functional reconstitution of purified sodium channels from rat brain and eel electric organ has also been achieved (Rosenberg et al., 1984; Hartshone et al., 1985; Recio-Pinto et al., 1987).

In this report, we study single sodium channels from squid optic nerve membranes incorporated into planar lipid bilayers in the presence of BTX. The results are compared with other sodium channels incorporated into bilayers, and with those obtained in the squid axon by the cut-open axon technique. We conclude that BTX-modified sodium channels transferred to planar bilayers share most of the properties with BTX-modified sodium channels present in the membrane of the giant squid axon. A preliminary report of this work has been published (Latorre et al., 1987).

MATERIALS AND METHODS

Materials

Tetrodotoxin (TTX), obtained from Calbiochem-Behring Corp. (San Diego, CA), was stored in stock solutions containing 1 mM citrate, pH 5. BTX was the generous gift of Dr. John Daly, National Institutes of Health, Bethesda, MD. Phospholipids were obtained from Avanti Polar Lipids, Inc., Birmingham, AL. The alkali metal chlorides were obtained from Alpha Inorganics (Danvers, MA).

Plasma membrane vesicles were prepared from the optical nerves of the squid *Sepiotheutis sepioidea* at the Instituto Venezolano de Investigaciones Cientificas. The optic nerves were dissected out in 0.75 M sucrose and 10 mM Tris (pH 7.4), and stored overnight in -20° . The purification of membrane vesicles was conducted according to Condrescu et al. (1984). For a number of reasons, the optic nerves of the squid represents a particularly suitable material, which yields numerous advantages such as no myelin contamination and a favorable ratio of

axonal over glial cells. The usual yield of the method is 2–3 mg of membrane per gram of wet nerve tissue.

Lipid Bilayers and Channel Incorporation

Lipid bilayers made from a solution of brain phosphatidylethanolamine, or its synthetic analogue 1-palmitoyl-2-oleoyl-phosphatidylethanolamine were formed in small holes (150–300 μm in diameter) in polystyrene partitions. The phospholipid was dissolved in decane to a final concentration of 15 mg/ml. Incorporation of channels was improved by imposing an ionic gradient across the bilayer, making the side in which the vesicles were added hyperosmotic. For incorporation of sodium channels, bilayers were formed in the presence of a 205-nM NaCl/5-mM NaCl gradient, and BTX was added to the high concentration side to a final concentration of 100 nM. 5–10 μl of the membrane vesicles were added to the BTX-containing compartment (compartment volume was 3 ml). Once a sodium channel was transferred to the planar bilayer, represented by a stepwise increase in current (~ 2 pA at 0 mV), the ionic gradient was dissipated and the channel orientation could be determined by its voltage dependence. In the presence of BTX the channels close at high hyperpolarizing potentials. Unless otherwise indicated the aqueous solutions were composed of NaCl at the desired concentrations plus 5 mM MOPS, pH 7. Experiments were done at 21–25°C.

Electrical Measurements and Data Analysis

The current passing through the membrane was measured with a two-electrode voltage clamp (Alvarez et al., 1985). Contacts with the aqueous solutions were made through silver/silver chloride electrodes connected to 0.2-M-NaCl agar bridges. One compartment was connected to a waveform generator and the other to a current-to-voltage converter (Burr-Brown OPA 101 operational amplifier; Burr-Brown Corp.; Tucson, AZ) with a feedback resistor of 1 G Ω . Because of the large membrane capacitance of bilayers (150–300 pF) the frequency response of the current-to-voltage converter is limited to ~ 300 Hz. For applied voltages the electrophysiological convention is used here. The aqueous phase to which the TTX-sensitive (external) side of the channel is facing is defined as zero voltage.

Single-channel currents were stored in a digital tape (Bezanilla, 1985*b*) for subsequent transfer to a digital computer for analysis of channel conductance, analysis of dwell times, and probability of opening (P_o). Before the analysis, current records were filtered with a digital eight-pole filter. Single-channel conductance was determined from the slope of the current-voltage relationship for the open channel. Distribution of open and closed times and P_o were analyzed from records filtered at 500 Hz. Since the voltage-to-current converter is essentially a one-pole filter, setting the digital filter at 500 Hz helps to eliminate high-frequency noise without altering the time response at which the records were originally taken. Mean open and closed times were obtained from linear dwell-time histograms and/or logarithmic histograms as described by Sigworth and Sine (1987). P_o was calculated by dividing the time the channel dwells in the open state and the total time of the current record.

TTX interaction with the channel occurs on a much lower time scale (seconds) than does channel opening and closing in the absence of this toxin. Consequently, as has been documented in detail (Moczydlowski et al., 1984*a*; Green et al., 1987*b*), the long quiescent periods representing channel blockade by TTX could be reliably distinguished from the short-lived closing events by setting a cutoff time of 300–600 ms. The rates of TTX interaction with the channel were measured by analyzing the slow transitions between open (unblock) or blocked periods. Long-lived closing events were also observed in the absence of TTX although they were of shorter mean duration than the TTX-induced blocked periods. These “spontaneous” closings, because they are produced much less frequently than the event induced by TTX, did

not introduce much error in the calculation of the rates of TTX binding and dissociation from sodium channels. Since the TTX block of squid optic nerve is very slow (mean blocked time ~ 70 s), we were able to obtain the rate constants for the blocking process only for two single-channel membranes. This fact also forced us to base the calculations on only 40–90 events.

RESULTS

Characteristics of BTX-activated Sodium Channels

Fig. 1 shows recordings obtained in three different membranes each containing a single BTX-activated channel. These records illustrate the most common modes of gating of squid optic nerve sodium channels found in these conditions. The top trace is part of a record lasting for 3 min. Single-channel current records showed

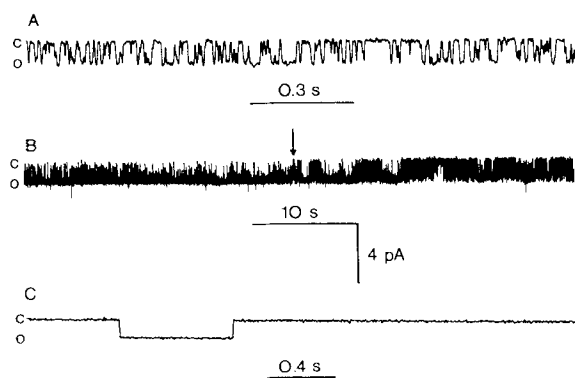


FIGURE 1. Examples of gating kinetics of single sodium channels. *c* indicates closed and *o* open. (A) Stationary gating kinetics. The holding potential was -90 mV. (B) Non-stationary gating kinetics. The arrow (down) marks the time the record was divided to measure the P_o . The values were 0.90 before the arrow and 0.55 after the arrow. The holding potential was -90 mV. (C) Slow "spontaneous" closure at a holding potential of $+70$ mV. All records taken in symmetrical 200 mM NaCl and in the presence of 100 nM BTX.

transitions between an open (*o*) and a closed (*c*) state. Transitions to subconductance states (i.e., channels showing a conductance that is a fraction of the one obtained from the top record of Fig. 1), were seldom seen (cf. Green et al., 1987a). During the entire length period of the record (3 min), channel gating kinetics was stationary and this was the type of records that we used to obtain kinetic parameters and P_o 's. In $\sim 5\%$ of the records a very different channel behavior was found (Fig. 1, middle trace). Here gating activity is characterized by sudden shifts in gating activity. In particular the shift in P_o marked by the arrow in the middle trace of Fig. 1, meant a change from a P_o of 0.90 to 0.55, as if the activation curve had shifted by ~ 20 mV. This type of gating behavior has been observed previously with glutamate channels (Gration et al., 1981), calcium-activated potassium channels (Moczydlowski and Latorre, 1983), and with muscle membrane BTX-activated sodium channels (Moczydlowski et al., 1984a). We also observed long-lasting closing events (bottom trace) that could be up to 1–2 s.

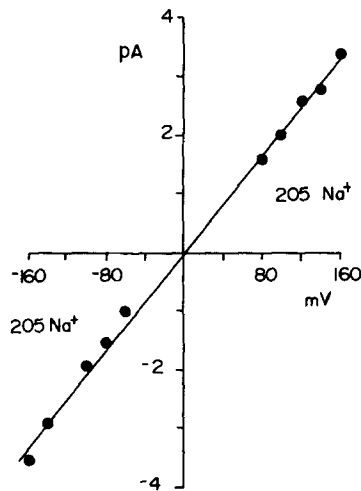


FIGURE 2. I-V relation for the open channel. Open-channel currents were measured in a bilayer containing a single sodium channel in 200 mM NaCl and 10 mM MOPS-NaOH, pH 7. The conductance calculated from the slope of the straight line was 20 pS.

Single-Channel Conductance

The size of the current jumps were obtained directly from records like the one shown in Fig 1 A, or by adding TTX to the external side to resolve fluctuations in current with reasonable residence times in the open and closed levels. The use of TTX was particularly useful at relatively large depolarizations where transitions to the closed state were seldom seen in the absence of this toxin.

In symmetrical 205 mM sodium the current-voltage (I-V) relationship for the open channel was linear in the voltage range of -160 to 160 mV (Fig. 2). The slope of the straight line gave a channel conductance of 20 pS. The average conductance obtained at this sodium concentration $[Na^+]$ was 20 ± 1 pS (mean \pm SEM from seven different single-channel membranes). I-V relationships like the one shown in Fig. 2 were determined at each $[Na^+]$ and conductances were determined from the slopes. At all $[Na^+]$ (range 5–540 mM Na^+) and between -80 and 80 mV I-V, relationships were linear. The experiment of Fig. 3 shows that the conductance vs. concentration data are well described by a simple rectangular hyperbola. The data can be fit to a hyperbola of the form $g = g_{max}[Na^+]/(K_m + [Na^+])$; where g is the chan-

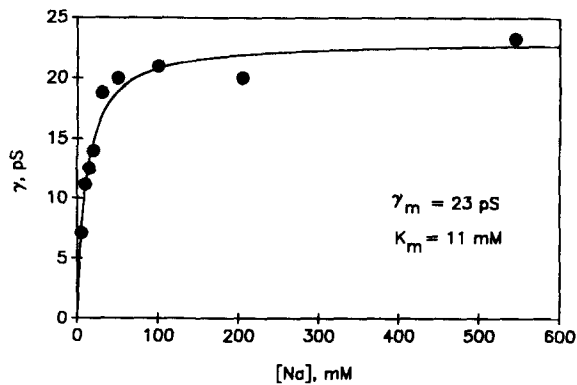


FIGURE 3. Single-channel conductance as a function of $[Na^+]$. Channel conductance (g) was measured as the slope of the I-V relations obtained at the indicated symmetrical $[Na^+]$. The curve is a fit to a rectangular hyperbola with a maximal conductance of 23 pS (g_{max}) and an apparent dissociation constant of 11 mM (K_m).

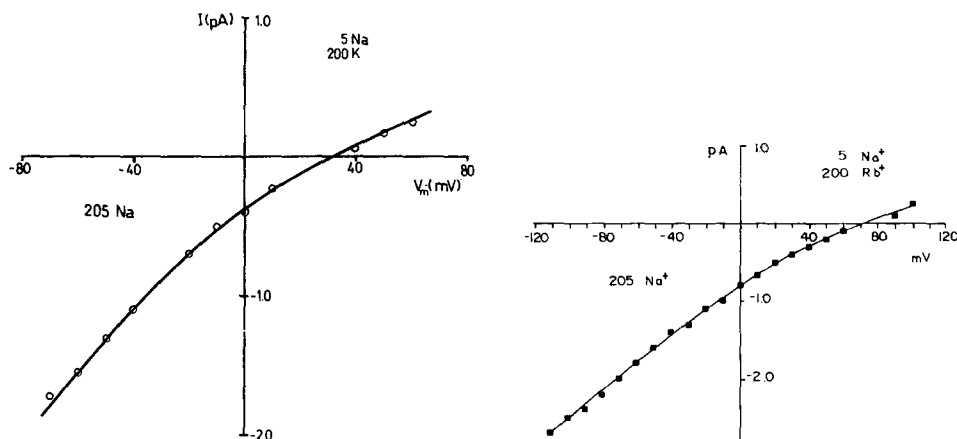


FIGURE 4. I-V relations in mixed ionic conditions. (A) The external side contained 200 mM NaCl and 10 mM MOPS-NaOH, pH 7. The internal side contained 200 mM KCl and 10 mM MOPS-NaOH, pH 7. The reversal potential was 33.5 mV. (B) External side as in A. Internal side: 200 mM RbCl and 10 mM MOPS-NaOH. Reversal potential was 73 mV.

nel conductance, g_{\max} denotes the maximal conductance observed at high $[\text{Na}^+]$, and K_m is the $[\text{Na}^+]$ at which the half maximal conductance is obtained. The fit gives a K_m of 11 mM and a g_{\max} of 23 pS. All the data points shown in Fig. 3 have been normalized to 23.5°C using a Q_{10} of 1.37 (Horn et al., 1984).

Ion Selectivity

The ion selectivity of BTX-activated sodium channels was determined by measuring reversal potentials under mixed-ion conditions (Fig. 4). Reversal potentials were determined from single-channel current curves, as illustrated in Figs. 4, A and B. In this case the external side contained 205 mM Na^+ and the internal side contained 200 mM of the test cation plus 5 mM Na^+ . As a rule the test cation was always added

TABLE I
Sodium Channel Permeability Ratios

Ion	$P_{\text{Na}}/P_{\text{ion}}$	
	Optic nerve (this work)	Squid axon (no BTX)
Na^+	1	1
Li^+	~1	
NH_4^+	1.4	3.7*
K^+	4.0	12.0 [†]
Rb^+	29.3	40.0 [‡]
Cs^+	>51	61.0 [‡]

The permeability ratios were calculated from bionic potentials. The aqueous solutions contained 205 mM Na^+ on the external side and 5 mM Na^+ and 200 mM of the test cation on the internal side. The anion was Cl^- .

*Binstock and Lecar, 1969.

†Chandler and Meves, 1965.

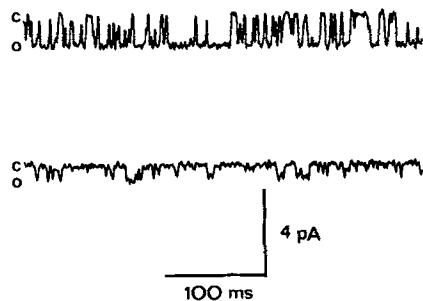


FIGURE 5. The effect of extracellular calcium on single sodium channels. Single-channel current fluctuations were measured in the absence (top trace) or in the presence of 10 mM Ca^{2+} (bottom trace). Channel current records were obtained at -90 mV and in symmetrical 200 mM Na^+ . The data were filtered at 150 Hz.

to the internal aqueous compartment. The reversal potential obtained from Fig. 4, *A* and *B* are 33.5 and 73 mV, respectively. Values for $P_{\text{Na}}/P_{\text{X}}$ were obtained using the Goldman-Hodgkin-Katz equation (Hodgkin and Katz, 1949) and by appropriately compensating for liquid-junction potentials. Reversal potentials and permeability ratios for the different alkali cations are given in Table I. The selectivity sequence obtained is $\text{Na}^+ \sim \text{Li}^+ > \text{NH}_4^+ > \text{K}^+ > \text{Rb}^+ > \text{Cs}^+$.

Divalent Cation Effects

Fig. 5 shows the effect of extracellular calcium addition on single sodium channel currents. At -80 mV the channel dwells most of the time in the open configuration. The addition of 10 mM Ca^{2+} , the $[\text{Ca}^{2+}]$ in sea water, had the effect of shifting the P_o toward more depolarized voltages and promoted a reduction in the channel conductance (Fig. 5). Fig. 6 shows the I-V relationship obtained in the absence (open symbols) and in the presence (closed symbols) of 10 mM Ca^{2+} and 50 mM Mg^{2+} in the external side. It is clear that the inward current is reduced by the presence of the divalent cations in the extracellular side. In this condition channel conductance is ~ 2 pS at potentials more negative than -20 mV (Fig. 6). Reduction in the open-channel current induced by these divalent cations is probably due to a fast voltage-dependent block. Blockade was relieved when the membrane was depolarized. Extracellular calcium block of BTX-modified rat brain sodium channels has been documented by Worley et al. (1986) and was interpreted as calcium binding to a site located at $\sim 23\%$ of the electrical distance from the extracellular surface.

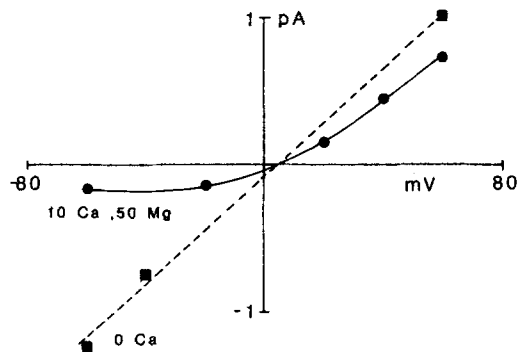


FIGURE 6. I-V relations in the absence and presence of divalent cations. A single sodium channel was incorporated in the presence of symmetrical 200 mM Na^+ and the I-V relation was determined (squares). The slope conductance was 19 pS. Solid circles represent channel currents obtained in the same membrane, but the external side contained 200 mM Na^+ , 50 mM Mg^{2+} , and 10 mM Ca^{2+} .

Voltage Dependence and Gating Kinetics

Fig. 7 illustrates typical current records obtained in a bilayer containing a single BTX-activated sodium channel of the squid optic nerve. The channel remains open most of the time at positive voltages to -60 mV, it is open 50% of the time at ~ -90 mV, and the channel is nearly always closed at voltages negative to -110 mV. Fig. 8 shows the P_o as a function of voltage. A steep voltage dependence of the activation curve is observed, similar to that of unmodified sodium channels. We tried to fit the data shown in Fig. 8 to a simple Boltzmann distribution derived for a two-state model, but while the fit was quite good for small P_o 's (below $P_o = 0.5$; dotted line in Fig. 8), the two-state model predicted P_o values that were consistently larger for P_o 's > 0.7 than the experimental data. The solid line is a fit to the P_o data using the expression:

$$P_o = 1 / \{1 + \exp[-z_2 F(V - V_2)/RT] [1 + \exp(-z_1 F\{V - V_1\}/RT)]\}. \quad (1)$$

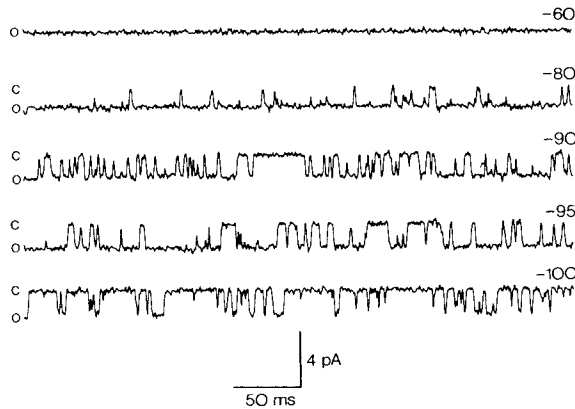
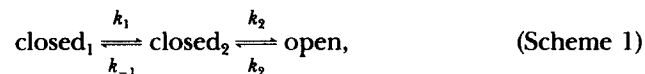


FIGURE 7. Current records of a single BTX-modified sodium channel. Holding voltages are shown at the right-hand side of the records, and *c* and *o* indicate the closed and open states, respectively. The aqueous phase was made up of 200 mM NaCl and 10 mM MOPS-NaOH, pH 7.

Eq. 1 corresponds to the P_o derived from the kinetic scheme:

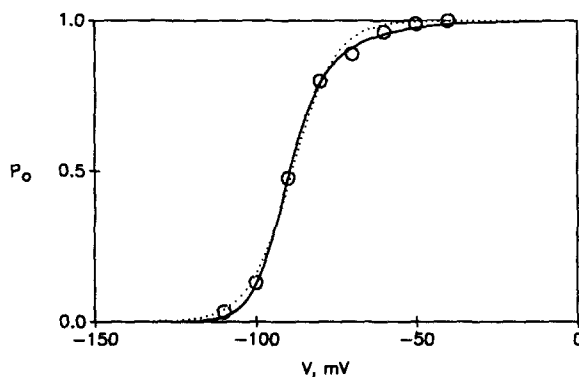


where z_1 and z_2 are the equivalent number of gating particles translocated during the closed-closed and the closed-open reactions, respectively. The total effective gating charge of the reaction is, therefore, $z_1 + z_2$, V_1 is the applied voltage at which $k_1/k_{-1} = 1$, V_2 is the voltage at which $k_2/k_{-2} = 1$, and R , T , and F have their usual meanings. In Fig. 8 P_o increases an e-fold per 4.6 mV and the effective gating charge of the overall reaction is 5.4 electronic charges. If the kinetic scheme -1 is taken as a reasonable representation of the gating process for the sodium channel, from Eq. 1 we obtained that during the partial reaction closed-closed 3.73 electronic charges are displaced, and the closed-open process (requires the translocation of 1.65 electronic charges. The voltage at which the channels are open 50% of the time, a value useful to compare with other preparations, is -90 mV.

Fig. 9 shows the effect of the addition of 10 mM Ca^{2+} to the external aqueous

solution that contained 205 mM Na⁺ on P_o (see also Fig. 5). The addition of calcium causes the P_o vs. V curve to shift to the right along the voltage axis without changing the voltage dependence. The shift amounts to 15 mV and we found effective gating charges of 4.8 and 4.25 in the absence and presence of calcium, respectively. This effect of external calcium on the sodium channel kinetic properties was first described in the squid giant axon by Frankenhaeuser and Hodgkin (1957), and more recently in sodium channel incorporated into bilayers (French et al., 1986b). The most simple explanation to this effect is a change in the intramembrane electric

FIGURE 8. Voltage dependence of BTX-modified sodium channel opening. The fraction of time the channel was open was determined by dividing the time the channel was open by the total time of the record. Symbols correspond to data points from a single-channel bilayer. The aqueous phase was made up of 200 mM NaCl and 10 mM MOPS-NaOH, pH 7. The dotted line was drawn through the data using the



expression $P_o = 1 / \{1 + \exp[zF(V - V_o)/RT]\}$, where z is the apparent gating charge and V_o is the voltage at which channels are open 50% of the time. The best fit was obtained with a V_o of -88.8 mV and a z of 3.7 electronic charge/channel. The smooth curve was drawn according to Eq. 1 of the text, which can also be written as $P_o = 1 / \{1 + (k_{-2}/k_2)[1 + (k_{-1}/k_1)]\}$. Parameters were found by fitting the above expression to the experimental data and the dwell times of Fig. 11 A using a nonlinear least-square method. The fitted rate constants are (in units of s⁻¹):

$$k_1 = 2,871 \exp [3.72F(V + 84.7)/RT]$$

$$k_2 = 696 \exp [0.03F(V + 104.6)/RT]$$

$$k_{-1} = 2,871 \exp [-0.016F(V + 84.7)/RT]$$

$$k_{-2} = 696 \exp [-1.62F(V + 104.6)/RT]$$

field arising as a consequence of the screening of fix negative charges in or near the external surface of the channel.

Probability density distributions of dwell times were constructed to obtain the characteristic time constants for the distribution of open and closed times. Furthermore, the goodness of the linear histogram fit was checked by constructing logarithmic histograms (Sigworth and Sine, 1987). Open-time distributions were well described by single exponentials (Fig. 10 A). For the example shown in Fig. 10 A, the solid line represents the fit of a single exponential to the data. Fitting was accomplished using a nonlinear least-squares routine. This suggests that there is only one open state and that the mean open time (T_o) is given by (see scheme 1):

$$T_o = 1/k_{-2} \quad (2)$$

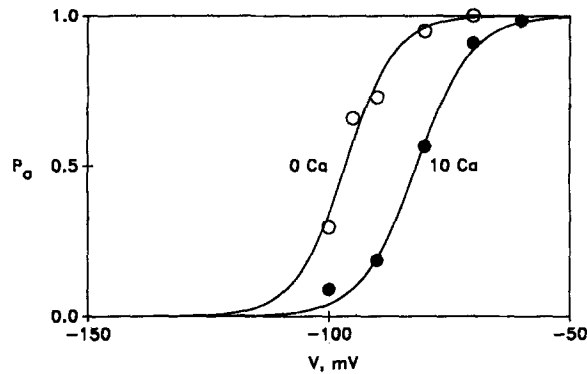


FIGURE 9. Effect of calcium on the fractional open time vs. voltage relation. A single sodium channel was incorporated into a bilayer separating identical 200 NaCl, 10 mM MOPS-NaOH solutions and P_o was measured at the indicated voltages (open circles). Upon the addition of 10 mM calcium to the extracellular side, a new P_o vs. V curve was taken (solid circles). The voltages at which the P_o was 0.5 were -97 and -82 mV, and the apparent gating charges were 4.8 and 4.25 in the absence and in the presence of calcium, respectively.

For closed-state dwell we also found single-exponential fits. At one voltage (-100 mV) two exponentials were necessary to fit the data. Time constants for these processes were 18 and 36 ms, the slow component accounting for only 10% of the total number of transitions (1,981). At potentials more positive than -70 mV a very fast component was apparent but not well resolved. In neuroblastoma cells and rat brain synaptosomes sodium channels a sum of two exponentials was required to fit the data for potentials > -80 mV (Huang et al., 1984, French et al., 1986*b*). As discussed by French et al. (1986*b*), the fact that we can approximate the closed dwell time distributions by a single exponential may result from reaction steps with similar life times. In our case we can be losing the slow components due to their small amplitude or we can be missing a component too fast to be captured by the current-to-voltage amplifier.

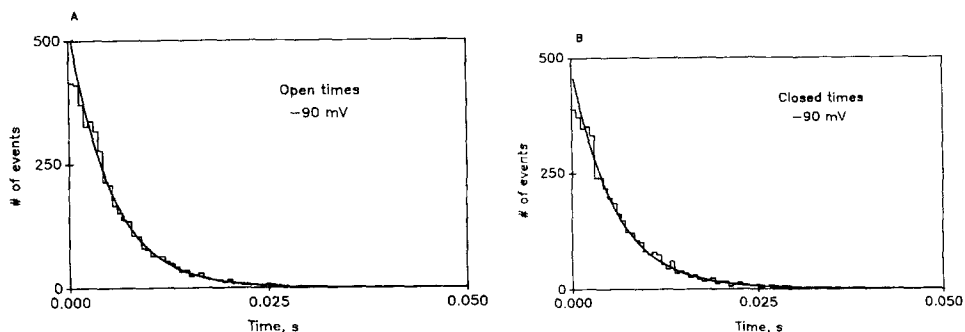


FIGURE 10. Probability density distribution of dwell times. Events were collected into bins of 0.6-ms width. The solid curves are least-square estimates (A) Open-time distributions. Time constant for the smooth curve is 5.2 ms. The holding voltage was -90 mV. (B) Closed-time distributions. Time constant for the smooth curve is 5.7 ms. Holding voltage -90 mV. The aqueous phase was 200 mM NaCl and 10 mM MOPS-NaOH, pH 7.

The dependence of mean open and closed times on membrane potential is shown in Fig. 11 A. The mean open times have an exponential dependence on voltage. In the present experiments the mean lifetime of the open state changed by e-fold for 16 mV change in voltage. However, we found that the mean closed times did not change in an exponential fashion with voltage, and large departures from a straight line were found when log mean closed times were plotted vs. applied voltage. For a closed-open kinetic scheme, exponential functions of voltage are expected for both mean open and closed times. Thus, our data are more consistent with the linear scheme 1. Fig. 11 B shows the log mean open and closed times vs. voltage relations in the absence (open symbols) and in the presence (closed symbols) of 10 mM Ca^{2+} . A parallel shift along the voltage axis was found for mean closed and open times.

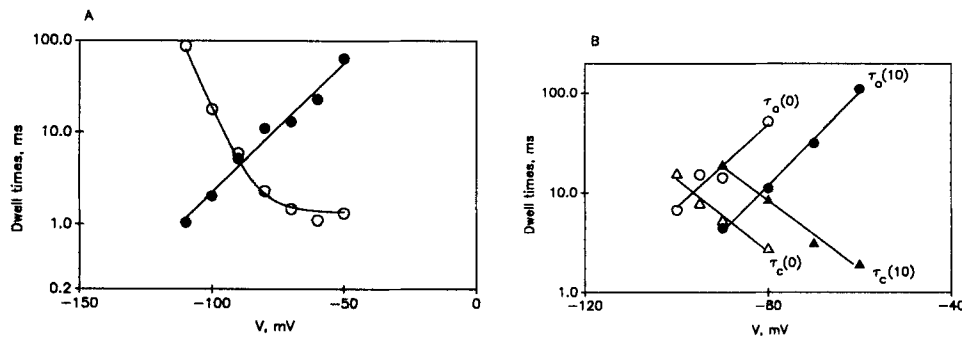


FIGURE 11. Voltage dependence of mean open and closed times. (A) The straight line is the linear regression line through the open-time data, using the equation $T_o = 1.43 \exp[1.62F(V + 104.6)/RT]$ in units of milliseconds. Closed times are the result of fitting the closed-time distributions. At potentials more positive than -70 mV a fast exponential component was found but the value plotted here is the slower component even though its amplitude is smaller. The data were fitted to

$$T_c = 2/[k_2 + k_1 + k_{-1} + \sqrt{(k_2 + k_1 + k_{-1})^2 - 4k_2k_1}],$$

which is one of the two eigenvalues of the three state model (Huang et al., 1984). The other eigenvalue is extremely fast and it would be undetected or at best distorted by our measurement system. Data from the same experiment shown in Fig. 8. (B) Effect of calcium on the mean open and closed times vs. voltage relations. Open symbols are data obtained in symmetrical 200 mM NaCl and closed symbols are data obtained after the addition of 10 mM Ca^{2+} in the external side. Numbers in parentheses indicate calcium concentration.

TTX Blockade

Fig. 12 shows records of a single activated sodium channel in the presence of TTX added to the extracellular side of the channel. Long-lived closing events were observed (note the differences in time scales compared with Fig. 7). These particular records were filtered at 2 Hz so the fast closing events were eliminated. Very long-lived channel closures induced by TTX have been found in several different BTX-activated sodium channels (Krueger et al., 1983; Moczydlowski et al., 1984a, b; Green et al., 1987b). No toxin-induced closures were present when the toxin was added to the intracellular side of the channel. Furthermore, TTX has no effect on

the frequency or duration of the events seen in the absence of this toxin. Since the residence time of the toxin in the channel was found to be very long (see below), it was very difficult to obtain experiments with a sufficient number of blocking events to analyze the kinetics of TTX blockade. The kinetics of TTX blockade were analyzed on the basis of two single-channel membranes. Although it is in principle possible to obtain the kinetic parameters for blockade in multi-channel membranes, we did not use this approach because we found that BTX-modified channels disappear spontaneously. Therefore, it is difficult, in multi-channel membranes, to be certain of the exact number of sodium channels. Spontaneous disappearance of dog brain BTX-modified sodium channels have been reported by Green et al. (1987a). They found that BTX-modified sodium channels disappear at a rate of 0.004 min^{-1} .

Fig. 13 shows the cumulative dwell time histograms for the open and blocked channel after the exclusion of rapid gating events at -40 and 40 mV. Both blocked

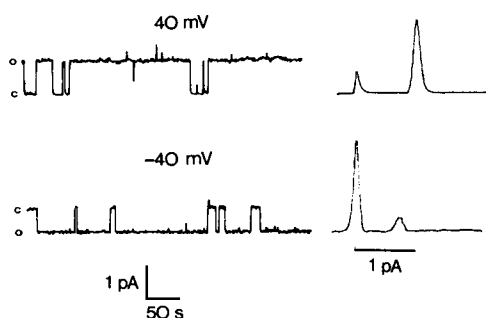
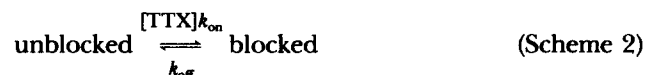


FIGURE 12. Discrete TTX block of a single sodium channel. Aqueous phase was 200 mM NaCl and 10 mM MOPS-NaOH; TTX was added to the external side only to a final concentration of 20 nM. The arrow indicates the blocked state. Current amplitude histograms are shown at the right-hand side of the figure. P_o was 0.84 at $+40$ mV and 0.15 at -40 mV. The slight difference in current amplitudes between the $+40$ and the -40 mV records correspond to the presence of a small sodium gradient across the bilayer. The data were filtered at 2 Hz.

and unblocked states exhibit single-exponential probability distributions. Therefore, the toxin-binding reaction can be approximated by the kinetic scheme:



where the unblocked state includes the open and closed states of the BTX-modified channel (Moczydlowski et al., 1984a). According to scheme 2, the second-order rate constant of blocking k_{on} , and on the first-order rate constant of unblocking k_{off} , can be defined as

$$k_{\text{on}} = 1/T_u[\text{TTX}] \quad (4)$$

$$k_{\text{off}} = 1/T_b \quad (5)$$

$$K_D = k_{\text{off}}/k_{\text{on}} \quad (6)$$

where T_u is the unblock mean time, T_b is the block mean time, and K_D is the dissociation constant. The rate constants calculated through Eqs. 4 and 5 using the T_u and T_b obtained from Fig. 13 are given in Table II. The results shown in Figs. 12,

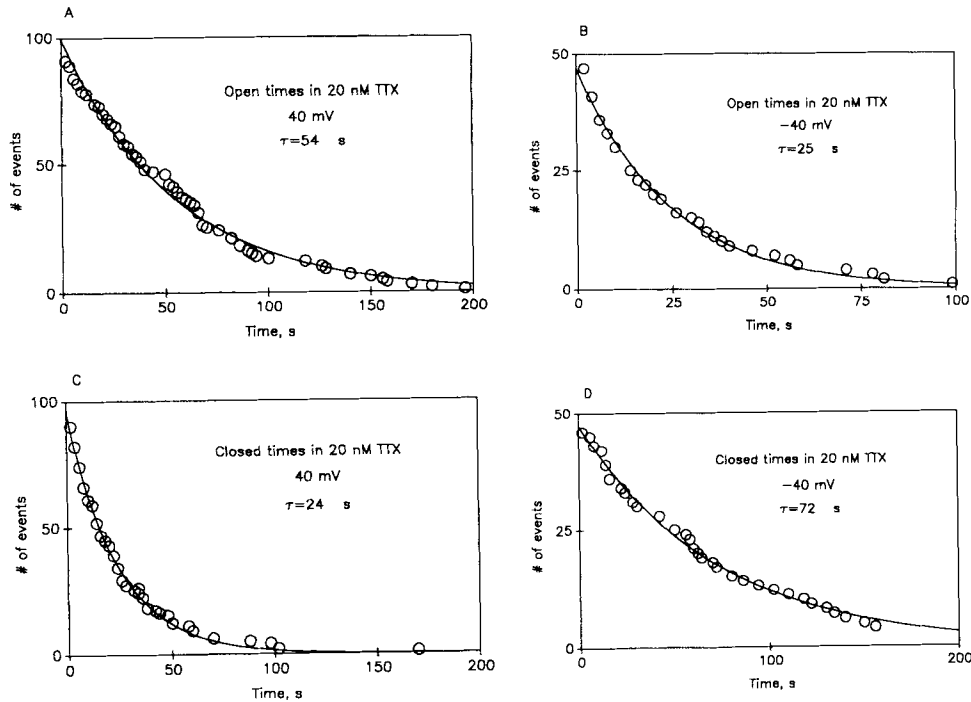


FIGURE 13. Cumulative dwell-time histograms in the presence of TTX. (A) Unblocked dwell times at +40 mV. (B) Blocked dwell times at +40 mV. (C) Unblocked dwell times at -40 mV. (D) Blocked dwell times at -40 mV. Solid lines represent exponential fits to the data. Aqueous phase was 200 mM NaCl and 10 mM MOPS-NaOH; TTX was added to a final concentration of 20 nM to the external side only.

13, and Table II indicate that blockade induced by TTX is voltage dependent (French et al., 1984; Moczydlowski et al., 1984a, b; Green et al., 1987b). K_D can be approximated to a exponential function of voltage according to the equation:

$$K_D(V) = K_D(0) \exp(AV). \quad (7)$$

Using the results shown in Table II the K_D interpolated to zero voltage was 16.4 nM. This value is similar to those found in rat and brain BTX-modified sodium channels (Moczydlowski et al., 1984b; Green et al., 1987b). However, the individual rate constants k_{on} and k_{off} are about 10-fold smaller. The mean blocked time in our experiments, interpolated to zero voltage, is 60 s, compared with a value of 10 s in rat muscle sodium channels (Moczydlowski et al., 1984b).

TABLE II
Kinetic Constants for TTX Blockade

V	TTX	T_b	k_{off}	T_u	k_{on}	K_D
mV	nM	s	s^{-1}	s	$s^{-1}M^{-1}$	nM
40	20	24	0.0417	54	9.26×10^5	45
-40	20	72	0.0139	25	2×10^6	6

DISCUSSION

Muscle and nerve membranes have been used as the preferred source of sodium channels for reconstitution studies in bilayers. However, the question of whether these channels present the same properties that they have when contained in the cellular membrane has remained unanswered because comparisons have been made using different preparations. We show below that BTX-modified sodium channels in bilayers and BTX-modified channels detected in the squid giant axon by means of the cut-open axon technique share most of their characteristics.

Channel Conductance

The average conductance we found for the optic nerve sodium channel in 200 mM Na^+ (20 pS) is very similar to that previously described for BTX-modified sodium channels in bilayers (Krueger et al., 1983, Moczydlowski et al., 1984a; Green et al., 1987a; Recio-Pinto et al., 1987). However, this value is higher than the values obtained in the squid giant axon by noise analysis (2–3.5 pS; Conti et al., 1975) or by the study of nonstationary noise of a small population of sodium channels in the cut-open axon (Llano and Bezanilla, 1984). Taking into account that the sea water used in the squid giant axon experiments contained a high concentration of divalent cations and considering the finding that calcium blocks sodium channels, low channel conductances are expected. In fact, by mimicking the divalent cation composition of sea water, we found that the BTX-modified sodium channel conductance is reduced to ~ 2 pS for potentials < -20 mV. More recently, Correa and Bezanilla (1988) reported that in the absence of divalent cations, BTX-modified sodium channels recorded from the giant squid axon by means of the cut-open axon technique have a conductance of 10 pS at 5°C in symmetrical 540 mM Na^+ . This value is comparable to the one obtained in the present work if a Q_{10} of 1.37 (Horn et al., 1984) for the channel conductance is considered. At 23.5°C the calculated conductance for the BTX-modified squid giant axon sodium channel is 18 pS. This value is 20% lower than the one obtained in the present work. The reasons for this discrepancy are not clear but a definite conclusion could only be drawn after the measuring of the conductance is done in the cut-open axon at high temperature.

We found that the single-channel conductance vs. $[\text{Na}^+]$ relation is well described by a Langmuir isotherm. This is the behavior expected for channels that can be occupied by, at most, a single ion (Lauger, 1973). Similar results have been obtained for the rat brain and rat muscle sodium channels. Both the affinity of the optic nerve sodium channel for sodium and the maximal conductance are very close to those obtained for rat muscle sodium channels ($K_m = 7$ mM, $g_{\max} = 22$ pS; Moczydlowski et al., 1984a; Garber and Miller, 1987), but lower than those obtained for the rat brain sodium channel ($K_m = 37$ mM, $g_{\max} = 31$ pS; French et al., 1986a). On the other hand, the conductance- $[\text{Na}^+]$ relation cannot be described by a rectangular hyperbola for dog brain (Green et al., 1987a) and for frog muscle BTX-modified sodium channels (D. Naranjo, O. Alvarez, and R. Latorre, unpublished results). As suggested by Green et al. (1987a) the departure from a simple Michaelis-Menten type of saturation isotherm can be accounted for by a net negative charge located at the channel entrance. A net negative charge in the conduction system of the pore will change the local accumulation of sodium in this region. The $[\text{Na}^+]$ at the chan-

nel entrance will be larger than in the bulk solution. Thus, it appears that there are sodium channel subtypes regarding their conductance- $[\text{Na}^+]$ behavior as there are subtypes regarding toxin binding (Barchi, 1987). It is possible that these subtypes contain different surface charge densities in the neighborhood of the channel entrances.

Surprisingly, the affinity of the squid optic nerve BTX-modified sodium channel for sodium is much larger than that obtained for the squid giant axon sodium channel. Apparent dissociation constants of 0.4–1 M for this channel have been obtained (Begenisich and Cahalan, 1980; Yamamoto et al., 1985). This discrepancy may arise, however, from the different ionic conditions used. Thus, the data for the giant axon sodium channel was obtained using a mixture of ions at a constant ionic strength. In their work they used tetramethylammonium (TMA) inside and Tris outside. TMA has a blocking effect on the sodium channel (Horn et al., 1981) and the replacement of sodium by Tris makes the blocking of calcium more effective in addition to the blocking effect of Tris. It is clear that calcium competes for occupancy of the channel and ionic competition should, in principle, reduce the apparent affinity of the channel for sodium (French et al., 1896*a*). A simple calculation based on competition of sodium and calcium for a blocking site gives a smaller apparent affinity constant, i.e.:

$$K_{\text{Na}}([\text{Ca}] = 50 \text{ mM}) = K_{\text{Na}}([\text{Ca}] = 0) (1 + [\text{Ca}]/K_{\text{Ca}}) \quad (8)$$

with a K_{Ca} of 6 mM obtained from the I-V curve in Fig. 6, we get $K_{\text{Na}}(50) = 100$ mM. Tris and TMA are expected to increase this value even more.

Channel Selectivity

The $P_{\text{Na}}/P_{\text{K}}$ value we obtained is lower than the one obtained for other sodium channels incorporated into planar bilayers and for the unmodified squid axon sodium channel (Table I). Values for this ratio vary in bilayers from 14.3 (Krueger et al., 1983; Moczydlowski et al., 1984*a*) to 5.5 (Green et al., 1987*a*). A value of 4.7 has been recently reported for purified eel electroplax sodium channels (Recio-Pinto et al., 1987). For the squid giant axon sodium channel this ratio is 12 (Table I; Chandler and Meves, 1965). The low value we obtained for the $P_{\text{Na}}/P_{\text{K}}$ can be the result of an asymmetry in the sodium channel permeation pathway (Cahalan and Begenisich, 1976; Garber and Miller, 1987). Thus, Garber and Miller (1987) have reported that the reversal potential decreased from 57 mV, obtained with a gradient $\text{Na}_{\text{in}}/\text{K}_{\text{out}}$ to 35 mV when the gradient was $\text{Na}_{\text{out}}/\text{K}_{\text{in}}$. This last value is very similar to the one we have obtained in the present work. However, we cannot discard at present the possibility that BTX-modified channels are less selective than unmodified channels. A lower alkali cation selectivity was found for the BTX-modified node of Ranvier sodium channel (Khodorov and Revenko, 1979) and in BTX-activated channels from neuroblastoma cells (Huang et al., 1979). It is interesting to note also that although the $P_{\text{Na}}/P_{\text{Li}}$ is very close to one, the slope conductances for these two ions are quite different. Thus, channel conductance for sodium and lithium in 200-mM ionic strength are 20 and 10 pS, respectively. Apparently, lithium binds more tightly to the sodium channel than sodium does.

Channel Gating

In the presence of BTX, sodium channels from the squid optic nerve are open 50% of the time at voltages ranging from -90 to -100 mV. Occasionally, we found channels that were activated at larger hyperpolarizations. On the other hand, the apparent gating charge that would have to move during the open-closed transition varied between 4 and 5. Our parameter values are very similar to those determined by Moczydlowski et al. (1984a) for rat muscle channels, by French et al. (1984, 1986b) for rat brain channels, and by Hatshorne et al. (1985) for purified channels from rat brain. In the cut-open axon, BTX-modified sodium channels show that the P_o vs. voltage relation is sigmoidal with a value of 0.5 at ~ -60 mV when calcium and magnesium are present (Llano and Bezanilla, 1986), but this voltage is shifted to ~ -80 when divalent cations are excluded from the artificial sea water (Correa and Bezanilla, 1988). Furthermore, the apparent gating charge determined from the P_o vs. voltage relations was determined to be ~ 4 . We also found a shift in the activation curves promoted by calcium of a magnitude similar to the one found in the giant axon (see Fig. 9, A and B). Both the P_o vs. voltage relation and the rate constants are shifted toward the right along the voltage axis upon the addition of calcium to the external side in a manner consistent with a surface charge effect. A net negative charge located near the channel gating machinery will give rise to a potential difference between the bulk aqueous phase and the gating machinery region. Calcium will screen these charges and hence will reduce this potential difference. One of the predictions of this simple model to explain the effect of calcium on channel gating is that opening and closing rate constants vs. voltage relations should be shifted in equal amounts along the voltage axis. This prediction is confirmed experimentally (Fig. 11 B).

Our kinetic results are consistent with a reaction scheme containing a single open state and several closed states. For channels containing only one open state the rate of closing from the open state, k_{-2} , is given by $k_{-2} = 1/T_o$ (Eq. 2). The mean open time shows an exponential dependence on voltage and it changed by an e-fold for ~ 16 mV. This result can be used to estimate the gating charge associated with channel closing (French et al., 1986b). A charge of 1.6 e/channel for the unidirectional closing step is needed to explain the voltage dependence of the mean open times. From Fig. 8 and Eq. 1 we obtained that 1.69 electronic charges are involved in the closed-open transition, which implies that a very small or no charge is associated with closed to open transition. Furthermore, the fact that only part of the total apparent gating charge can be associated with the closed-open reaction gives further support that there are more than one closed state connected by voltage-dependent rate constants.

The four rate constants were estimated using the P_o vs. V curve and the dwell times vs. V curves, and they were assumed to be exponential function of voltages. The expressions obtained are in the figure legend of Fig. 8. The results indicate very small voltage dependence in the closed₂ to open transition as compared with the closed₁ to closed₂ transition. In addition, k_1 and k_{-2} are more voltage dependent than k_{-1} and k_2 . These results are different from the rates reported by Huang et al. (1984) in neuroblastoma cells or by Keller et al. (1986) in purified sodium channels.

The time resolution of the present experiments is too limited to decide whether these differences are significant.

We thank Dr. J. Daly for his generous gift of BTX. We thank Dr. M. Condrescu and Dr. R. DiPolo for providing us with membrane preparation from the retinal nerve. Dr. DiPolo contributed in some of the preliminary experiments.

This work was supported by National Science Foundation INT-8610434, the Fondo Nacional de Investigacion grant 0483-1987, National Institutes of Health grants GM-35981 and GM-30376, and by a grant from the Tinker Foundation.

Original version received 21 March 1988 and accepted version received 22 July 1988.

Note added in proof: A. M. Correa, R. Latorre, and F. Bezanilla (*Biophysical Journal*, 1989, in press) have measured a conductance of 18.3 pS for the BTX-treated Na channel in the cut-open squid axon at 22°C.

REFERENCES

- Alvarez, O., D. Benos, and R. Latorre. 1985. The study of ion channels in planar bilayer membranes. *Journal of Electrophysiological Techniques*. 12:159-177.
- Armstrong, C. M. 1981. Sodium channels and gating currents. *Physiological Reviews*. 61:644-683.
- Barchi, R. L. 1987. Sodium channel diversity: subtle variations on a complex theme. *Trends in Neurosciences*. 10:221-223.
- Begenisich, T., and M. D. Cahalan. 1980. Sodium channel permeation in squid axons. Nonindependence and current-voltage relations. *Journal of Physiology*. 307:243-257.
- Bezanilla, F. 1985a. Gating of sodium and potassium channels. *Journal of Membrane Biology*. 88:97-111.
- Bezanilla, F. 1985b. A high capacity data recording device based on a digital audio processor and a video cassette recorder. *Biophysical Journal*. 47:437-441.
- Bezanilla, F. 1987. Single sodium channels from the squid giant axon. *Biophysical Journal*. 52:1087-1090.
- Binstock, L., and H. Lecar. 1969. Ammonium currents in the squid giant axon. *Journal of General Physiology*. 53:342-361.
- Cahalan, M. D., and T. Begenisich. 1976. Sodium channel selectivity. Dependence on internal ion concentration. *Journal of General Physiology*. 68:111-125.
- Chandler, W. K., and H. Meves. 1965. Voltage clamp experiments on internally perfused giant axons. *Journal of Physiology*. 180:788-820.
- Condrescu, M., L. Osses, and R. DiPolo. 1984. Partial purification and characterization of the (Ca + Mg)-ATPase from optic nerve plasma membrane. *Biochimica et Biophysica Acta*. 769:261-269.
- Conti, F., L. J. De Felice, and E. Wanke. 1975. Potassium and sodium ion current noise in the membrane of the squid axon. *Journal of Physiology*. 248:45-82.
- Correa, A. M., and F. Bezanilla. 1988. Properties of BTX-treated single Na channels in squid axon. *Biophysical Journal*. 53:226a. (Abstr.)
- Frankenhaeuser, B., and A. L. Hodgkin. 1957. The action of calcium on the electrical properties of squid axons. *Journal of Physiology*. 137:218-244.
- French, R. J., B. K. Krueger, and J. F. Worley. 1986a. From brain to bilayer. Sodium channels from rat neurons incorporated into planar lipid membranes. In: *Ionic Channels in Cells and Model Systems*. R. Latorre, editor. Plenum Press, N.Y. 273-290.

- French, R. J., J. F. Worley, M. B. Blaustein, W. O. Romine, K. K. Tam, and B. Krueger. 1986b. Gating of batrachotoxin-activated sodium channels in lipid bilayers. *In* Ion Channel Reconstitution. C. Miller, editor. Plenum Press, New York. 363–383.
- French, R. J., J. F. Worley, and B. K. Krueger. 1984. Voltage-dependent block by saxitoxin of sodium channels incorporated into planar lipid bilayer. *Biophysical Journal*. 45:301–310.
- Garber, S. S., and C. Miller. 1987. Single Na⁺ channels activated by veratridine and batrachotoxin. *Journal of General Physiology*. 89:459–480.
- Gration, K. A. F., J. J. Lambert, G. Ramsey, and P. N. R. Usherwood. 1981. Non-random openings and concentration dependent lifetimes of glutamate-gated channels in muscle membranes. *Nature*. 291:423–425.
- Green, W. N., L. B. Weiss, and O. S. Andersen. 1984. Batrachotoxin-modified sodium channels in lipid bilayers. *Annals of the New York Academy of Sciences*. 435:548–550.
- Green, W. N., L. B. Weiss, and O. S. Andersen. 1987a. Batrachotoxin-modified sodium channels in lipid bilayers. Ion permeation and block. *Journal of General Physiology*. 89:841–872.
- Green, W. N., L. B. Weiss, O. S. Andersen. 1987b. Batrachotoxin-modified sodium channels in lipid bilayers. Characterization of saxitoxin- and tetrodotoxin-induced closures. *Journal of General Physiology*. 89:873–903.
- Hartshorne, R. P., B. U. Keller, J. A. Talvenheimo, W. A. Catterall, and M. Montal. 1985. Functional reconstitution of the brain sodium channel into planar lipid bilayers. *Proceedings of the National Academy of Sciences*. 82:240–244.
- Hodgkin, A. L., and A. F. Huxley. 1952. A quantitative description of the membrane current and its application to conduction and excitation in nerve. *Journal of Physiology*. 117:500–544.
- Hodgkin, A. L., and B. Katz. 1949. The effect of sodium ions on the electrical activity of the giant axon of the squid. *Journal of Physiology*. 108:37–77.
- Horn, R., J. Patlak, and C. F. Stevens. 1981. The effect of tetramethylammonium on single sodium channel currents. *Biophysical Journal*. 36:321–327.
- Horn, R., C. A. Vanderberg, and K. Lange. 1984. Statistical analysis of single sodium channels. *Biophysical Journal*. 45:323–335.
- Huang, L. M., W. A. Catterall, and G. Ehrenstein. 1979. Comparison of ionic selectivity of batrachotoxin-activated channels with different tetrodotoxin dissociation constants. *Journal of General Physiology*. 73:839–854.
- Huang, L. M., N. Moran, and G. Ehrenstein. 1984. Gating kinetics of batrachotoxin-modified sodium channels in neuroblastoma cells determined from single channel measurements. *Biophysical Journal*. 45:313–322.
- Keller, B. U., R. P. Hartshorne, J. A. Talvenheimo, W. A. Catterall, and M. Montal. 1986. Sodium channels in planar lipid bilayers. Channel gating kinetics of purified sodium channels modified by batrachotoxin. *Journal of General Physiology*. 88:1–23.
- Khodorov, B. I. 1985. Batrachotoxin as a tool to study voltage-sensitive sodium channels of excitable membranes. *Progress in Biophysics and Molecular Biology*. 45:57–148.
- Khodorov, B. I., and S. V. Revenko. 1979. Further analysis of the mechanisms of action of batrachotoxin on the membrane of myelinated nerve. *Neuroscience*. 4:1315–1330.
- Krueger, B. K., J. F. Worley, and R. J. French. 1983. Single sodium channel from rat brain incorporated into planar lipid bilayer membranes. *Nature*. 303:172–175.
- Latorre, R., A. Oberhauser, M. Condrescu, and R. DiPolo. 1987. Incorporation of sodium channels from squid optic nerve into planar bilayers. *Biophysical Journal*. 51:195a. (Abstr.)
- Lauger, P. 1973. Ion transport through pores: a rate theory analysis. *Biochimica et Biophysica Acta*. 311:423–441.

- Llano, I., and F. Bezanilla. 1984. Analysis of sodium current fluctuations in the cut-open squid giant axon. *Journal of General Physiology*. 83:133–142.
- Llano, I., and F. Bezanilla. 1986. Batrachotoxin-modified single sodium channels in squid axon. *Biophysical Journal*. 49:43a. (Abstr.)
- Moczydlowski, E., S. S. Garber, and C. Miller. 1984a. Batrachotoxin-activated Na⁺ channels in planar lipid bilayers. Competition of tetrodotoxin block by Na⁺. *Journal of General Physiology*. 84:665–686.
- Moczydlowski, E., S. Hall, S. S. Garber, G. S. Strichartz, and C. Miller. 1984b. Voltage-dependent blockade of muscle Na⁺ channels by guanidinium toxins. Effect of toxin charge. *Journal of General Physiology*. 84:687–704.
- Moczydlowski, E., and R. Latorre. 1983. Gating kinetics of Ca²⁺-activated K⁺ channels from rat muscle incorporated into planar lipid bilayers. Evidence for two voltage-dependent binding reactions. *Journal of General Physiology*. 82:511–542.
- Recio-Pinto, E., D. S. Duch, S. R. Levinson, and B. W. Urban. 1987. Purified and unpurified sodium channels from the eel electroplax in planar lipid bilayers. *Journal of General Physiology*. 90:375–395.
- Rosenberg, R. L., S. Tomiko, and W. S. Agnew. 1984. Single channel properties of voltage-regulated Na channels isolated from the electroplax of *Electrophorus electricus*. *Proceedings of the National Academy of Sciences*. 81:5594–5598.
- Sigworth, F. J., and S. M. Sine. 1987. Display and fitting of single-channel dwell time histograms. *Biophysical Journal*. 52:1047–1054.
- Worley, J. F., R. J. French, and B. K. Krueger. 1986. Trimethylxonium modification of single batrachotoxin-activated sodium channels in planar bilayers. Changes in unit conductance and in block by saxitoxin and calcium. *Journal of General Physiology*. 87:327–349.
- Yamamoto, D. J., Z. Yeh, and T. Narahashi. 1985. Interaction of permeant cations with sodium channels of squid axon membranes. *Biophysical Journal*. 48:361–368.